International Journal of Humanoid Robotics
Vol. 4, No. 3 (2007) 487–506

World Scientific
www.worldscientific.com

A QUASI-PASSIVE LEG EXOSKELETON FOR LOAD-CARRYING AUGMENTATION

CONOR JAMES WALSH[*,§], KEN ENDO[†,¶]
and HUGH HERR[‡,‖,**]

[*]*Department of Mechanical Engineering,*
MIT, 77 Massachusetts Avenue,
Cambridge, MA 02139, USA

[†]*MIT Media Lab, 20 Ames Street,*
Cambridge, MA 02139, USA

[‡]*MIT-Harvard Division of Health Sciences and Technology,*
Cambridge, MA 02139, USA
[§]*walshcj@mit.edu*
[¶]*kene@media.mit.edu*
[‖]*hherr@media.mit.edu*

Received 16 January 2007
Revised 8 March 2007

A quasi-passive leg exoskeleton is presented for load-carrying augmentation during walking. The exoskeleton has no actuators, only ankle and hip springs and a knee variable-damper. Without a payload, the exoskeleton weighs 11.7 kg and requires only 2 Watts of electrical power during loaded walking. For a 36 kg payload, we demonstrate that the quasi-passive exoskeleton transfers on average 80% of the load to the ground during the single support phase of walking. By measuring the rate of oxygen consumption on a study participant walking at a self-selected speed, we find that the exoskeleton slightly increases the walking metabolic cost of transport (COT) as compared to a standard loaded backpack (10% increase). However, a similar exoskeleton without joint springs or damping control (zero-impedance exoskeleton) is found to increase COT by 23% compared to the loaded backpack, highlighting the benefits of passive and quasi-passive joint mechanisms in the design of efficient, low-mass leg exoskeletons.

Keywords: Exoskeleton; walking; load-carrying; springs.

1. Introduction

As compared to wheeled vehicles, exoskeleton-based assistive devices have several potential advantages, such as allowing the user to traverse irregular terrain surfaces. Individuals employed in particular recreational, occupational and military activities often carry heavy loads using a variety of backpack systems. Recreational hikers commonly carry subsistence and comfort items in backpacks.[1] Fire fighters and other emergency personnel also use backpack systems to carry oxygen tanks and

**Corresponding author: MIT Media Lab, Room E15-424.

other equipment.[2] Still further, foot soldiers often carry heavy backpack loads and walk long distances across rough terrain.[1]

A leg exoskeleton could benefit people who engage in load carrying by increasing load capacity, lessening the likelihood of leg or back injury, improving metabolic locomotory economy, or reducing the perceived level of difficulty. Exoskeletons have been developed that amplify human strength by applying assistive torques to the joints and/or by supporting a payload.[3–10] These investigations have focused on fully actuated systems that are often energetically expensive, requiring a large power supply with frequent refueling or recharging.

Alternatively, biomechanical investigations have shown that animal and human walking is very energy efficient due to energy storage strategies that are exploited to reduce muscle work.[11–14] The exchange between gravitational potential energy and kinetic energy of the center of mass (CM) suggests that CM dynamics during the single support phase in walking may be approximated as a passive mechanical process.[11] Further, muscle work required to swing the legs in walking is minimal because of a pendulum-like exchange of gravitational potential energy and limb kinetic energy.[12] Recent research indicates that elastic energy storage is also critical for stable and economical bipedal walking.[13,14]

Can mechanical energy storage strategies be exploited in the design of prosthetic, robotic, and exoskeletal systems for walking? The use of passive and quasi-passive mechanisms that enhance mechanical energy exchange between elastic, gravitational and kinetic energy forms has been a key design paradigm for leg prostheses. Through this design strategy, the work from onboard actuators and/or from the wearer's own muscles can be effectively reduced, resulting in prosthetic systems that are lightweight, energy efficient, and operationally quiet. The majority of commercially available ankle-foot mechanisms comprise passive springs that store energy during early to mid stance, and release that energy to power terminal stance plantar flexion.[15] A number of knee prostheses use variable-damping mechanisms that output modest damping levels during much of the swing phase, allowing the prosthetic leg to freely swing so as to exploit natural swing-leg pendular mechanics. The knee devices then increase damping at heel strike and early stance, preventing the knee from buckling as weight is applied to the prosthesis.[16–20]

Passive dynamic walkers have also been constructed that rely on mechanical energy storage strategies.[21] In such bipedal systems, a human-like pair of legs settles into a natural gait pattern generated by the interaction of gravity and inertia. Similar to prosthetic leg designs, a knee clutch is employed to allow the leg to freely swing and then to keep the knee fully extended at heel strike and throughout early stance. Although a purely passive walker requires a modest incline to power its movements, researchers have enabled robots to walk across level ground surfaces by adding just a small amount of energy at the hip or ankle joint.[22,23]

Recently a quasi-passive exoskeleton was developed for load-carrying augmentation during level ground walking.[24–26] The device runs parallel to the legs, transferring payload forces worn on the back of the wearer to the ground. The exoskeletal system comprises elastic energy storage elements at the hip and ankle,

and a variable-damping mechanism at the knee. During metabolic evaluations, however, the exoskeleton was shown to *increase* walking metabolic power by 32% as compared to a standard loaded backpack using a 34 kg payload.[25] More recently, another quasi-passive exoskeletal design was constructed, and metabolic evaluations showed that the mechanism increased metabolic power by 60% on average compared to standard loaded backpack for 20 kg, 40 kg and 55 kg load configurations.[27]

The primary objective of this investigation is to advance a quasi-passive exoskeletal design for load carrying that achieves an improved walking metabolic performance as compared to a standard loaded backpack. We seek an exoskeletal design that comprises passive and quasi-passive mechanisms to enhance mechanical energy storage and exchange so as to minimize the work required by the wearer to drive the exoskeleton. To that end, we construct an exoskeleton that comprises a heel spring, a subtalar joint inversion/eversion spring, ankle dorsi/plantar flexion springs, a knee variable damper, and hip flexion and abduction springs. Exoskeletal spring stiffnesses are optimized using a human leg model and walking gait data. For a 36 kg payload, we hypothesize that a leg exoskeleton of this design will improve metabolic walking economy compared to a standard loaded backpack. We further hypothesize that the quasi-passive exoskeleton will improve walking economy compared to an exoskeleton without joint springs or damping control (zero joint-impedance exoskeleton). As a preliminary evaluation of these hypotheses, we measure the rate of oxygen consumption and carbon dioxide production to determine metabolic power of a study participant walking at a self-selected speed using the quasi-passive exoskeleton, the zero-impedance exoskeleton, and a standard loaded backpack.

2. Quasi-Passive Leg Model for Slow Walking

The first objective of this investigation was to construct an exoskeleton for load carrying augmentation that performed well at slow walking speeds (0.8–1 m/s). As a first step in the design process, the human leg was modeled using passive and quasi-passive joint mechanisms, or springs, clutches and variable-damping elements. Figure 1 shows the sagittal plane model employed for the exoskeletal design. Palmer showed that by characterizing the stance-phase behavior of the human ankle in terms of simple mechanical spring elements, sagittal plane dynamics of the joint could be reproduced at slow walking speeds.[28] Based on this result, series-elastic clutch elements were used to model effective ankle dorsi and plantar flexors. In addition, since knee mechanical power is largely negative throughout the gait cycle in human walking, especially at slow walking speeds, the knee was modeled as a variable damper.[29] Finally, motivated by the human leg model of Endo *et al.*, series-elastic clutch elements were used to model effective hip flexion/extension muscles.[14] The series-elastic clutches were used to control spring engagement times at the ankle and hip during the various phases of gait. In total, the leg model of Fig. 1 consists of eight series-elastic clutch parameters: four spring constants and four distinct times when clutches are engaged to begin energy storage and release cycles of the series

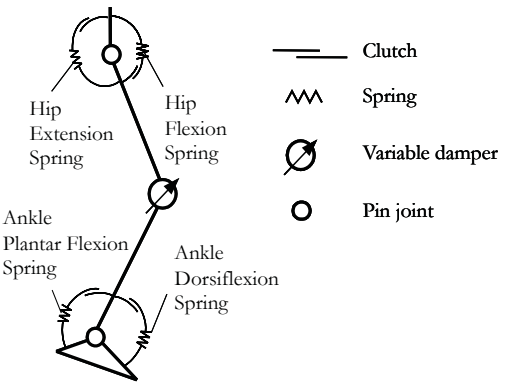

Fig. 1. Passive leg model for slow walking. The sagittal plane model comprises two monoarticular springs at the hip, a variable-damping device at the knee and two monoarticular springs at the ankle. There are no actuators included in the model.

springs. By convention, a flexion spring is a spring that promotes joint flexion upon elastic energy recoil.

To optimize these model parameters, human gait data were obtained from the literature.[28] Human data were joint angles, moments and powers from hip, knee and ankle in the sagittal plane. Data were for a 50 kg study participant with a 0.71 m leg length and a walking speed of 0.88 m/s. Data from this particular individual was obtained because the upper body mass was equal to 33 kg which was approximately equal to the 36 kg payload of the exoskeleton.

In the optimization strategy, the simplex search method was employed to find optimal spring constants and clutch engagement times. Optimization was conducted so as to minimize the fitness function representing the integral of the square error of moment during one step:

$$\text{fitness} = \sum_{\text{joint}} \int_t (\tau_{bj}(t) - \tau_{sj}(t))^2 dt, \tag{1}$$

where τ_{bj} and τ_{sj} denote the biological and simulated torque of joint j, respectively, and t is time. Figure 2 shows simulation results plotted against the human joint data. The results show that the ankle plantar flexor captures 93% of the negative work and 54% of positive work throughout the gait cycle. Furthermore, the hip flexor captures 96% of the negative work and 58% of positive work during the gait cycle. At the ankle, the spring constants obtained for the dorsi and plantar flexion springs were 50 Nm/rad and 341 Nm/rad, respectively. For the hip joint the values were 105 Nm/rad and 54 Nm/rad for the flexion and extension springs, respectively.

3. Quasi-Passive Exoskeletal Components

Motivated by the optimization results in Sec. 2, in this section we discuss the hardware implementation of the various quasi-passive joint mechanisms. The desired

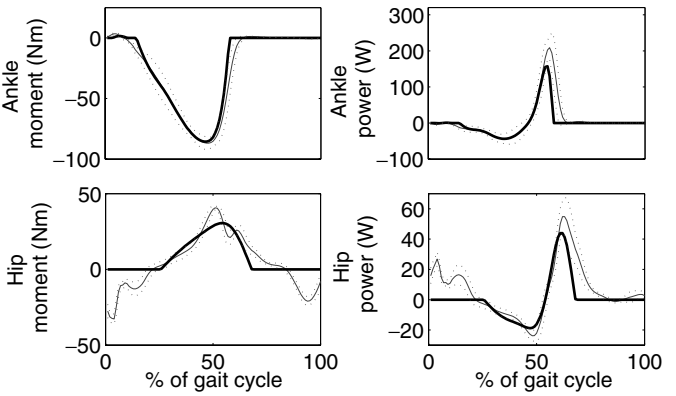

Fig. 2. Optimization results. The sagittal plane ankle and hip moment and power are plotted for the model and biological data. The solid thin line is the mean of the human gait data ($n = 7$ walking trials), and the dashed lines are one standard deviation about the mean. The solid thick line is the model or simulation curve. All curves start at heel strike (0% gait cycle) and end with the heel strike of the same leg (100% gait cycle).

rotary stiffnesses at the ankle and hip joints were implemented using linear springs compressed by levers. A variable damper was used at the knee joint and was programmed to exert desired damping levels throughout the walking cycle. Figure 3 shows the completed exoskeleton. Without the payload, the total mass of the exoskeleton was 11.7 kg. The masses of the various exoskeletal sections were as follows: lower leg section 1.46 kg, upper leg section 2.56 kg, pelvic harness, artificial spine and backpack mount 3.66 kg.

3.1. *Ankle and foot springs*

The ankle joint was implemented as a single degree of freedom (DOF) pin joint that was collocated with the human ankle joint. In addition, a compliant subtalar joint was implemented via a carbon fiber plate, connecting the exoskeletal leg with the boot of the wearer.

3.1.1. *Ankle dorsi and plantar flexion springs*

Dorsi and plantar flexion springs were designed as uni-directional elements wherein the sub-assembly could be adjusted to vary spring engagement angles. During the walking cycle, the plantar flexion spring stored energy during controlled dorsiflexion, and that energy was subsequently released to assist the human foot during powered plantar flexion. The dorsiflexion spring was compressed during controlled plantar flexion, as the foot was placed flat on the ground after heel strike, and that energy was then released to initiate controlled dorsiflexion. The optimization results of Fig. 2 were used to select spring stiffness values for dorsi and plantar flexion exoskeletal springs. The spring constants for the dorsi and plantar flexion

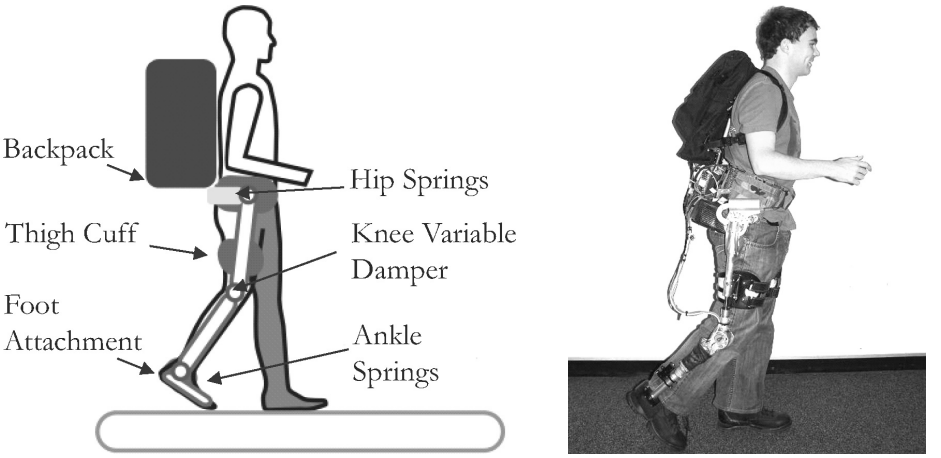

Fig. 3. Quasi-passive exoskeleton. In (a), the main interface and joint components of the exoskeleton are shown. The exoskeleton was designed to provide a parallel load path to transfer the weight of the backpack directly to the ground. A standard military issued backpack, Alice Pack, was selected to carry the load. A carbon fiber harness connected rigidly to the backpack frame to transfer the load from the backpack to the exoskeleton. The exoskeleton interfaced to the human via shoulder straps, a waist belt, thigh cuffs, and a shoe connection. The degrees of freedom were chosen to minimize kinematic constraints experienced by the wearer and joint ranges of motion accommodated normal human walking. Further, the physical connection between the exoskeleton and the human enabled the exoskeleton to passively track the human's leg motion. In (b), a participant is shown walking with the exoskeleton.

springs were 9.8 kN/m and 247 kN/m. The lever mechanism to transform the linear stiffness to effective rotary stiffnesses at the ankle joint (see Fig. 4) had a moment arm of 3.8 cm, giving effective rotary stiffnesses of 14 Nm/rad and 343 Nm/rad for dorsi and plantar flexion springs, respectively. During system evaluations, the wearer found that a lower stiffness of 14 Nm/rad for the dorsiflexion spring was preferable over the leg model value of 50 Nm/rad.

3.1.2. *Subtalar joint inversion/eversion and heel springs*

The exoskeletal leg attached to a modified boot through a sagittally-aligned carbon fiber plate that also served as a subtalar joint inversion/eversion spring. Figure 4 shows the subtalar joint spring. The subtalar spring permitted transverse rotation of the leg, reducing parasitic forces on the wearer's foot during walking. Figure 4 also shows a carbon fiber heel spring for energy storage and shock absorption, acting as an artificial heel pad. This spring reduced impact losses at heel strike, and aided in lifting the heel from the walking surface to initiate powered plantar flexion.

3.2. *Knee variable damper*

The exoskeletal knee joint was a single DOF pin joint collocated with the human knee. The knee mechanism comprised a magnetorheological (MR) damper with the

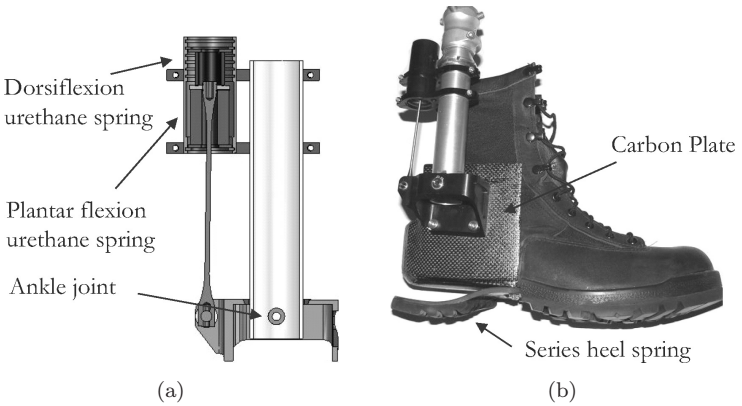

Fig. 4. Ankle and foot springs. In (a), a section view of the ankle joint sub-assembly is shown with two urethane springs. The dorsiflexion spring is compressed from heel strike to foot flat. The plantar flexion spring is engaged as the shin rocks forward during mid-stance. In (b), the ankle sub-assembly is shown attached to a modified military boot via a carbon plate for compliance for subtalar joint inversion/eversion.

MR fluid used in the shear mode, similar to that used for a prosthetic knee joint.[20] The knee variable damper could exert a maximum braking torque of 60 Nm and consumed on average 1 W of electrical power during walking. A current command from an amplifier powered an electromagnet that created a magnetic field across a stack of inter-spaced steel blades. Adjacent blade pairs rotated relative to one another as the knee was flexed, with one blade attached to the exoskeletal thigh section and the other adjacent blade attached to the exoskeletal lower-leg section. Between adjacent blade pairs was a 20 m MR fluid gap. The knee comprised 76 MR fluid gaps with a total of 77 blades. The knee architecture is shown in Fig. 5. A more comprehensive description of the knee mechanism can be found in the literature.[20]

Residual magnetism in the MR damper created a residual torque that impeded knee flexion/extension during the swing phase. As a resolution to this difficulty, the damper was demagnetized before every swing phase. The time available for demagnetization was approximately 200 ms. To meet this requirement, a current pulse opposite in sign to the magnetization current was sent through the device. For the specific MR damper employed in the exoskeleton, a pulse amplitude of 1 A and duration of 50 ms was used.

3.3. *Hip flexion and abduction springs*

The exoskeletal hip joint had two DOF to allow for hip flexion/extension and abduction/adduction movements. Medial/lateral rotation of the hip was facilitated using a yaw rotary joint located just above the exoskeletal knee. The flexion/extension hip DOF was collocated with the human hip. For the abduction/adduction DOF, a cam mechanism was designed to adjust the exoskeletal leg length during abduction/adduction hip movements.[26] The optimization results from

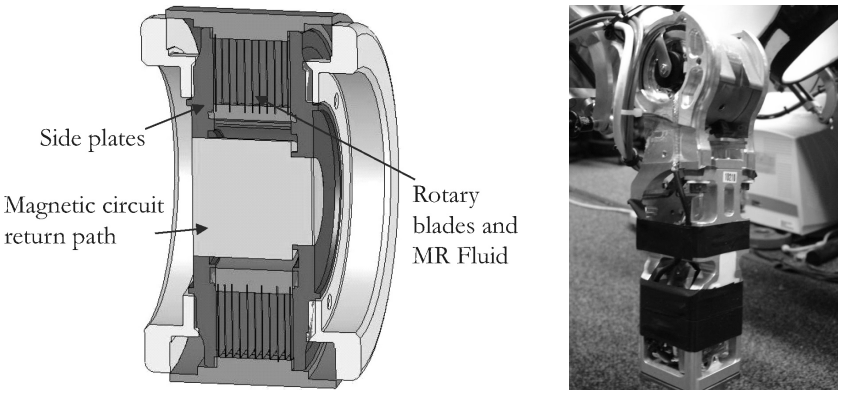

Fig. 5. Knee variable damper. In (a), a section view of the knee sub-assembly is shown. One set of blades are grounded to the outside shell and another to the inside. When the knee rotates adjacent upper and lower blades move relative to one another, shearing the MR fluid between the blades. Using an electromagnet around the return path, a magnetic field can be modulated through the rotary blade plus MR fluid gaps, so as to change knee damping. In (b), the knee variable damper is shown mounted on the exoskeleton leg.

Sec. 2 show that the hip flexion spring captures approximately three times more work than the hip extension spring. Thus, for the current exoskeleton, the extension spring was omitted to simplify the design.

3.3.1. *Hip flexion spring*

The hip flexion spring, shown in Fig. 6, was designed to be uni-directional to allow the wearer's hip to freely flex but to resist hip extension movements. The sub-assembly was designed to allow for easy adjustment of spring engagement angle. The hip flexion spring stored energy during hip extension and released that energy to assist hip flexion movements in walking. The hip spring was 3.8 cm in diameter, 10 cm in length with 5 cm of travel, and had a stiffness of 19.3 kN/m. A plunger, fixed to the exoskeletal leg, compressed the flexion spring. The flexion spring was enclosed in a casing attached to the exoskeletal harness to prevent the wearer's fingers from being pinched. A thin delrin plate covering the spring served as a low friction surface for contact with the plunger. The plunger had a moment arm of 7.6 cm, giving an effective rotary joint stiffness of 112 Nm/rad.

3.3.2. *Hip abduction spring*

When the wearer stood on one leg, the backpack load induced an anterior-posterior moment since the direction of the backpack load was off center from the biological hip joint. This moment was undesirable and caused discomfort to the wearer. To solve this problem, a linear compression spring (see Fig. 7) was placed at the

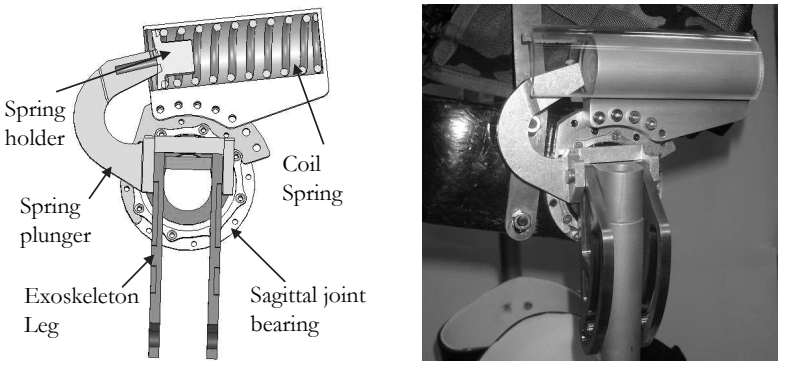

Fig. 6. Hip flexion spring. In (a), a section view of the hip flexion spring sub-assembly is shown. The spring plunger rotates in the sagittal plane with the exoskeletal leg. The plunger engages with a spring holder and energy is stored as the spring is compressed. In (b), the hip flexion spring assembly mounted on the exoskeleton is shown.

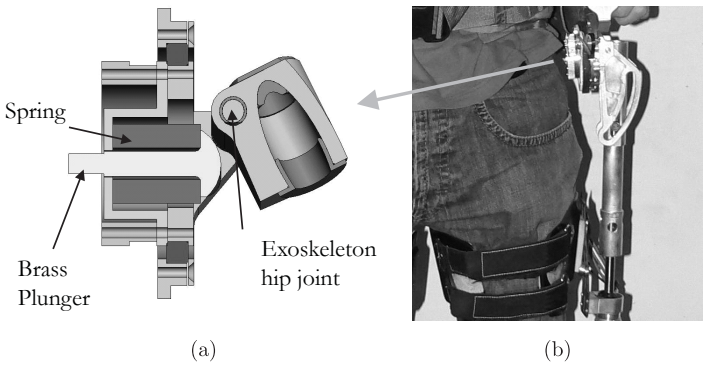

Fig. 7. Hip abduction spring. In (a), a coronal section drawing is shown of the abduction spring sub-assembly at the hip joint. It is uni-directional so it allows the leg to freely abduct. The spring is kept in place by means of a keeper that attaches to the exoskeletal hip joint assembly. The keeper is grounded to the sagittal plane bearing so that the keeper rotates with the exoskeletal leg. A brass plunger fits through a hollow spring, allowing the spring to be compressed during hip abduction. In (b), a view of the abduction spring location is shown on the exoskeletal leg.

exoskeletal hip abduction/adduction DOF. The abduction spring was unidirectional and only compressed during hip adduction. The wearer could freely abduct the exoskeletal hip joint without engaging the abduction spring. Thus, the spring only compressed during the stance phase when the leg underwent adduction. An effective rotary stiffness of 96 Nm/rad was required to counter the undesirable moment, and was obtained using a 425 kN/m linear spring compressed by a lever arm equal to 1.5 cm in length.

4. Electronics Hardware

4.1. *Electronics overview*

The exoskeleton was made autonomous by means of an onboard computer with a data acquisition card, power supply and amplifiers. The system was powered by a 48 V battery pack. A custom breakout board was designed to interface the sensors to the D/A board on a PC104, as well as to provide power to the signal conditioning boards. The amplifiers for the variable damper were 48 V digital amplifiers from Copley (Model No. ACK-090-04, Canton, MA). A schematic of the electronics setup showing the power and information flow is shown in Fig. 8.

4.2. *Exoskeletal sensors*

The transitions between the different phases of the gait cycle were detected using a combination of full-bridge strain gauges placed on the structure of the exoskeletal shank between the knee and ankle, and a rotary potentiometer at the knee joint. The strain gauges were used to measure the axial force and bending moment applied to the lower-leg exoskeletal section. In order to achieve an acceptable signal to noise ratio, the sensor raw voltage readings were amplified with a differential line driver, and the signal was then filtered with an analog low-pass filter with a cutoff frequency of 1.5 kHz.

5. Quasi-Passive Joint Mechanism Function

Figure 9 outlines the function of each of the quasi-passive joint mechanisms as a function of gait cycle. The exoskeletal knee is the only component that is actively controlled. The engagement angles for the hip and ankle springs were determined from the optimization results presented in Sec. 2.

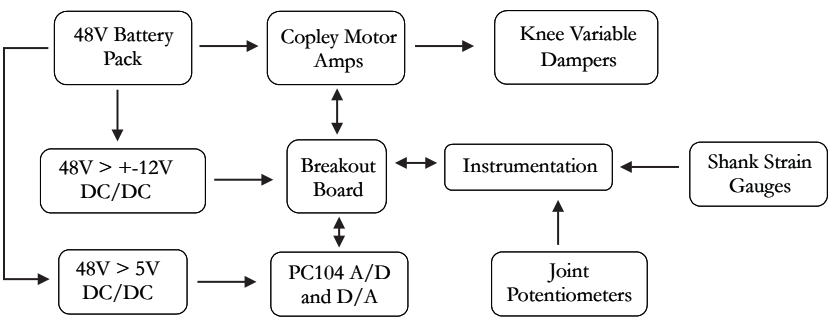

Fig. 8. Electronics schematic. The exoskeletal sensor data were recorded to a PC104 A/D card. The PC104 commanded a current from the Copley amplifiers that were used to power the knee variable damper. A custom breakout board was designed to interface with the PC104.

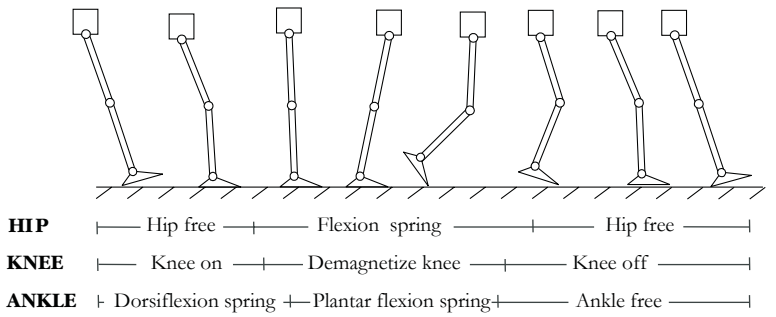

Fig. 9. Exoskeletal joint behavior. The sagittal plane joint behavior of the exoskeletal leg is shown from heel strike to the next heel strike of the same leg. The hip flexion spring is compressed during late-stance and this energy is released to assist the onset of the swing phase. At the knee, the damper mechanism is turned on at heel strike as the exoskeletal leg is loaded and turned off during terminal stance to allow knee flexion. The ankle dorsiflexion spring is compressed during controlled plantar flexion and the energy is then released during the beginning of controlled dorsiflexion. The plantar flexion spring engages in controlled dorsiflexion to store energy that is later released to assist in powered plantar flexion.

5.1. *Knee variable damping control*

The knee state-machine controller processed knee angle, force and moment measured from the exoskeletal leg to define four phases of the walking cycle. Knowledge of these states provided periods of the gait cycle when the desired action of the variable-damping mechanism was known. Table 1 lists the states and the sensory readings that were used as triggers to switch between states.

When the axial force measured by the strain gauges passed a set threshold, the knee entered the first state, *Stance*, where it was programmed to exert a torque proportional to knee rotational velocity. Two distinct damping constants were used for knee flexion and extension. *Pre-swing* was entered when the measured knee moment reached a certain threshold. During *Pre-swing* when the knee remained at full extension, knee demagnetization was implemented. *Swing Flexion* began when the load in the exoskeletal shank dropped to near zero, indicating the initiation of swing phase. The knee state-machine entered the final state *Swing Extension* when maximum knee flexion was reached. Throughout the entire swing phase, the damper was turned off so as to allow the knee to bend freely when the foot was no longer

Table 1. A description of states and their respective triggers for the state-machine of the knee controller.

State	Description	Trigger
0	Zero Damping	Load in exoskeleton leg
1	Stance	Load in exoskeleton leg
2	Pre-swing	Knee angle and moment in exoskeleton leg
3	Swing Flexion	Load in exoskeleton leg
4	Swing Extension	Knee angle

in contact with the ground surface. Further details of the control scheme employed for the exoskeleton can be found in the literature.[30]

6. Experimental Protocol

One male subject participated in the study (age 24; body weight 76 kg; leg length 0.93 m). The protocol was approved by MIT's Committee on the Use of Humans as Experimental Subjects (COUHES). The participant was a volunteer and was permitted to withdraw from the study at any time and for any reason. Before taking part in the study, the participant read and signed a statement acknowledging informed consent.

Four walking experiments were conducted using: (i) a standard loaded backpack, (ii) the quasi-passive exoskeleton, (iii) a zero-impedance exoskeleton, and (iv) a loaded backpack with the equivalent exoskeletal weight (11.7 kg) distributed across the participant's torso and legs (added-mass condition). For the *zero-impedance* exoskeletal condition, the hip flexion/abduction springs and ankle dorsi/plantar flexion springs were removed. In addition, no knee damping control was provided during the walking trial. For the *added-mass* experimental condition, the equivalent mass of the exoskeletal links, joints, plus the backpack were distributed at those locations on the participant's body equivalent to the CM of the respective exoskeletal section. For example, a weight equivalent to the exoskeletal thigh section mass was attached to the participant's thigh at the CM location of that section. For each experimental condition, the payload was chosen to be 36 kg, a value that is representative of a typical load carried by a service person.[31]

Before the study began, the participant had approximately 5 hours of acclimatization to the quasi-passive exoskeletal device. Before each experimental trial, the participant walked with each experimental condition for five minutes. The participant's self-selected walking speed was measured while wearing the quasi-passive exoskeleton. To control for walking speed between the exoskeletal conditions, the participant walked approximately 2 m behind a modified golf caddy set at the quasi-passive exoskeletal speed. The axial force measured from strain gauges within the exoskeletal leg was recorded to determine the percentage of exoskeletal weight plus payload transferred through the exoskeletal structure. In addition, participant oxygen intake and carbon dioxide production were measured. The participant was advised not to have intense or prolonged exercise for 24 hours prior to the experimental session. Further, the participant was instructed to stay hydrated and not to have caffeine or a large meal three hours before the experiment.

6.1. *Metabolic cost of transport estimate*

The energy cost was estimated from O_2 consumption and CO_2 production measured with a portable K4 telemetric system.[32] The K4 system included a portable unit worn by the participant, and a base station where data were recorded. The portable unit weighed 1.5 kg and consisted of a silicon mask containing a flow-rate

turbine that was fixed to the participant's face with a strap. A processing unit containing the O_2 and CO_2 analyzers was strapped to the subject's chest, and a transmitter/battery pack was placed inside the backpack.

Data collection spanned three days to avoid fatigue effects. Before each experimental session the turbine was calibrated with a three-liter syringe, and a two-point calibration of the O_2 and CO_2 analyzers was carried out using ambient air and a standard calibration gas mixture (5% CO_2, 16% O_2, 79% N_2). For each experimental trial, the participant walked around the MIT indoor track for ten minutes while $\dot{V}_{O_2}$ (the rate of oxygen consumption) and $\dot{V}_{CO_2}$ (the rate of carbon dioxide production) data were recorded. Rest measurements were taken while the participant was seated for 6 min before and after each walking trial. For all experiments performed, the respiratory exchange ratio (RER) was less than or equal to 1.0, indicating that energy was supplied primarily by oxidative mechanisms. The resting $\dot{V}_{O_2}$ and $\dot{V}_{CO_2}$ values were subtracted from the walking trial data. These values were then used to calculate metabolic power requirements for each walking condition using the following standard equation[3]:

$$\dot{E}_{\text{net metabolic}} = 16.68 \frac{W.s}{ml\text{O}_2} \dot{V}_{O_2} + 4.51 \frac{W.s}{ml\text{CO}_2} \dot{V}_{CO_2}. \tag{2}$$

The total cumulative energy for each walking trial was then plotted. When the data showed a line of constant slope, steady state energy consumption was assumed. The walking metabolic cost of transport (COT) for each trial was then calculated from the following formula:

$$\text{COT} = \frac{\text{Total Energy}}{\text{Distance Traveled} \times \text{Total Weight}}. \tag{3}$$

The total energy was calculated for a fixed period of time (3 min) after steady state had occurred. The total weight was equal to the weight of the exoskeletal system plus the participant. The distance traveled was obtained by multiplying walking speed by the time period for which the total energy was calculated, or 3 min.

7. Results

7.1. *Knee state-machine operation*

During the exoskeletal load-carrying experiments, the variable damper state machine performed robustly. Figure 10 shows real time data for a 12 s period of exoskeletal walking with the state (dashed line of arbitrary heights corresponding to states 0 through 4 in increasing magnitudes) superimposed over knee angle and axial force data. From the period of time between 7 and 10 s, it can be seen that the state-machine operates robustly even while the study participant is shuffling while turning around. After 7 s, the controller state goes back and forth between state zero, where the leg is off the ground, and state one, where the leg is on the

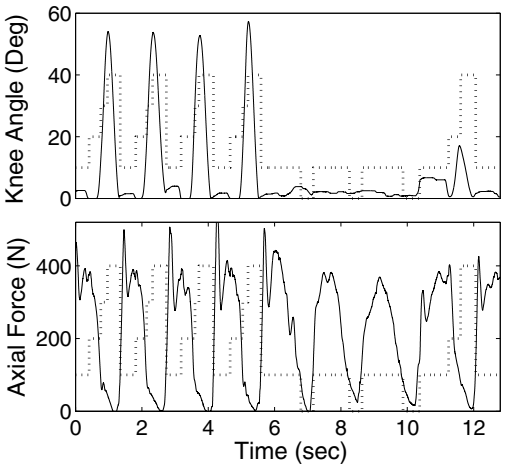

Fig. 10. Knee state machine operation. The exoskeletal knee angle and axial force are plotted with the knee state (dashed-line) superimposed on both plots. Knee state machine transitions performed robustly during exoskeleton operation. From 0 to 7 s, the participant is walking. After this walking period, he stops, turns around, and then resumes walking as indicated by a state sequencing of 1-2-3-4 beginning at approximately 10 s.

ground. When the participant begins walking again at approximately ten seconds, the controller once again cycles through the states associated with walking, or state sequence 1-2-3-4.

7.2. *Axial load transfer through the exoskeletal leg*

Figure 11 shows exoskeletal axial force, normalized by system weight, as a function of gait cycle. The data show only force information measured from one exoskeletal leg. The peak axial force at heel strike is 1.07 times exoskeletal weight (467 N). The data show that the exoskeleton does transfer loads to the ground with an average load transfer of 80% during the single support phase of walking, or from 15% to 55% gait cycle in Fig. 11.

7.3. *Walking metabolic COT*

For each of the four experimental conditions, the steady-state rate of metabolic energy consumption was determined by first plotting the total cumulative energy versus walking time. The data typically reached a constant slope after approximately 2 min from the start of the experiment, indicating that the rate of metabolic energy consumption had reached a steady state value. These data are shown in Fig. 12 for all four experimental conditions.

In Table 2, the metabolic power, total weight and COT for each experimental condition are listed. The self-selected walking speed for the quasi-passive exoskeleton was 0.92 m/s, and that same speed was used for the other experimental conditions.

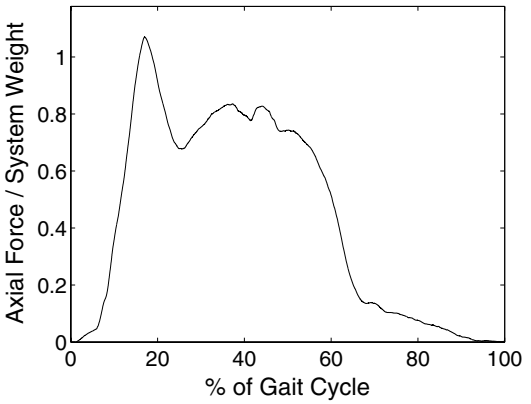

Fig. 11. Normalized axial force during walking. The normalized axial force is plotted from heel strike (0% gait cycle) to heel strike of the same leg (100% gait cycle). The axial force is normalized by the exoskeleton plus payload weight equal to 467 N.

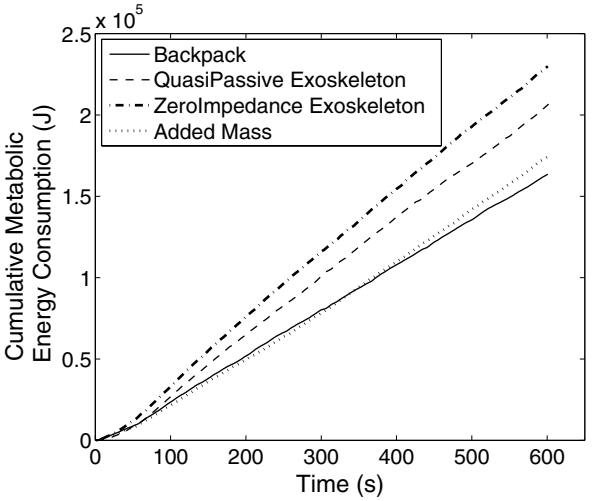

Fig. 12. Walking metabolic data. The total cumulative energy for each of the four experimental conditions are plotted, with a constant slope for each indicating that a constant rate of energy consumption is reached.

Table 2. Comparison of experimental conditions. The total weight, power and the COT, calculated using Eq. (3), are listed for each experimental condition.

Condition	Backpack	Quasi-Impedance Exo	Zero-Impedance Exo	Added-Mass
Total Weight (N)	1099	1216	1158	1216
Power (W)	277	344	383	291
COT	0.25	0.27	0.31	0.26

Although a significant fraction of the payload is transferred through the exoskeletal structure as shown in Fig. 11, the quasi-passive exoskeleton is found to increase metabolic COT by 10% compared to the standard loaded backpack. By comparing the quasi-passive exoskeleton to the zero-impedance exoskeleton, the relative effect of the ankle/hip springs and knee variable-damping components are determined. Metabolic data show that the zero-impedance exoskeleton increases metabolic COT by 23% compared to the loaded backpack, and 12% compared to the quasi-passive exoskeleton, highlighting the benefits of spring and variable-damping mechanisms at the ankle, knee and hip. Finally, the added-mass condition increases the COT by only 5% compared to the standard loaded backpack, suggesting that added mass alone cannot explain the 10% COT increase caused by the quasi-passive exoskeleton.

8. Discussion

Exoskeletons have been developed that amplify human strength by applying assistive torques to the joints and/or by supporting a payload for the wearer.[3–10] Many of these investigations have focused on fully actuated systems that are energetically expensive, requiring a large power supply with frequent refueling or recharging. In this investigation we ask whether energy storage strategies might be exploited to increase the economy of exoskeletal walking. To this end, we seek an exoskeletal design that comprises passive and quasi-passive mechanisms to enhance mechanical energy storage and exchange between the exoskeleton and the wearer. We construct an exoskeleton that comprises a heel spring, a subtalar joint inversion/eversion spring, ankle dorsi/plantar flexion springs, a knee variable damper, and hip flexion and abduction springs. By carefully selecting spring engagement joint angles and stiffnesses, we anticipate that the work output of the human ankle and hip can be effectively lowered during exoskeletal walking. Further, by controlling exoskeletal knee damping, we anticipate that the negative work requirements of the human knee can be effectively lowered. Our modeling results support these claims. Using a leg model and human gait data, we find optimal spring engagement angles and stiffnesses that maximally reduce joint work (see Sec. 2). In the leg model, the hip flexion spring captures 96% of the negative work and 58% of positive work during the human gait cycle. Further, the ankle plantar flexion spring captures 93% of the negative work and 54% of positive work performed during the stance period. Because of these large reductions in human joint work, we hypothesize that the quasi-passive exoskeleton will improve walking COT compared to an exoskeleton without ankle/hip joint springs or knee damping control (zero-impedance exoskeleton). Our preliminary metabolic data are in support of this hypothesis. We find that the zero-impedance exoskeleton increases metabolic COT by 12% compared to the quasi-passive exoskeleton.

Even though the 36 kg payload is largely supported by the exoskeletal structure during single support (see Fig. 11), the exoskeleton nonetheless increases the COT by 10% compared to the conventional loaded backpack. There are many potential

reasons why a quasi-passive leg exoskeleton might increase walking metabolism. The exoskeletal leg mass may increase the forces borne by the human body during leg accelerations. Another reason might be that the friction in the joints of the exoskeleton effectively increase the net positive work requirements of the human body. More likely is that the exoskeleton applies kinematic constraints on the human wearer due to poor collocation of the joints and/or a restrictive interface between the exoskeleton and operator, forcing an unnatural, inefficient movement pattern. It has been shown that changes in natural gait increase the physiological energy expended during locomotion.[34] Still further, the energies stored in the exoskeletal spring mechanisms might be released in a manner that causes the human wearer to select movement patterns that increase walking COT.

To better understand why the quasi-passive exoskeleton increases COT, two additional experiments are conducted. First, we measure the COT with only pin joints at the exoskeletal ankle, knee and hip, removing the ankle/hip springs and the knee damping control (zero-impedance exoskeleton). This zero-impedance exoskeleton, which was otherwise identical to the quasi-passive exoskeleton, increases the COT by 23% compared to the loaded backpack. Since removal of the joint springs and damping control increases the COT from 10% to 23% compared to the backpack case, we reason that the inclusion of these passive and quasi-passive mechanisms improves performance and is therefore not the cause of increased COT.

One might expect that the added mass and inertia itself might fully explain the COT increase of the quasi-passive system. However, as noted in the results (Sec. 7), the added-mass condition only increases the COT by 5% compared to the loaded backpack. What might be the cause for the 18% difference between the zero-impedance exoskeletal COT and the added mass COT? Since the joint springs are removed in the zero-impedance case, the increase in COT cannot be attributed to a destabilization of the wearer's walking pattern due to the release of stored elastic energy. Further, since active knee damping is not utilized on the zero-impedance exoskeleton and friction in the joints is minimized by the use of high-quality bearings, energy losses at the joints of the exoskeleton likely do not substantially contribute to the 18% increase in COT. We therefore conclude that the dominant causes for the observed COT increase are added mass and kinematic constraints imposed on the wearer.

9. Future Work

In future investigations, we wish to address the above shortcomings and fully realize a quasi-passive exoskeleton that decreases walking COT compared to a conventional loaded backpack. Given the results of this study, we believe that further increasing the amount of elastic energy storage while keeping exoskeletal mass low will be of critical importance. The use of exoskeletal bi-articular and mono-articular elastic structures that more closely mimic the human musculoskeletal leg architecture may be an important strategy for increasing mechanical energy storage and

exchange in exoskeletal walking.[14] Furthermore, since kinematic constraints due to poor exoskeletal joint collocation was a key factor in the results of this investigation, joint architectures that more closely track human movement patterns will be required. We believe that, in order to create highly functional leg exoskeletons, exoskeletal-joint collocation and mechanisms that promote mechanical energy exchange are critical design features.

Acknowledgments

This research was performed under Defense Advanced Research Projects Agency (DARPA) contract #NBCHC040122, *Leg Orthoses for Locomotory Endurance Amplification.*

References

1. C. Fletcher, *The Complete Walker* (Alfred Knopf, New York, 1974).
2. V. Louhevaara, J. Smolander, T. Tuomi, O. Korhonen and J. Jaakkola, Effects of an SCBA on breathing pattern, gas exchange, and heart rate during exercise, *J. Occup. Med.* **27** (1985) 213–216.
3. B. J. Makinson, Research and development prototype for machine augmentation of human strength and endurance, Hardiman I Prototype Project, Report S-71-1056 (General Electric Company, Schenectady, New York, 1971).
4. H. Kazarooni, The human power amplifier technology at the University of California, Berkeley, *J. Robot. Autonom. Syst.* **19** (1996) 179–187.
5. J. Pratt, B. Krupp, C. Morse and S. Collins, The RoboKnee: An exoskeleton for enhancing strength and endurance during walking, in *IEEE Int. Conf. Robotics and Automation (ICRA)*, New Orleans, USA (IEEE Press, 2006), pp. 2430–2435.
6. H. Kawamoto and Y. Sankai, EMG-based hybrid assistive leg for walking aid using feedforward controller, in *Int. Conf. Control, Automation and Systems*, Jeju, Korea (2001), pp. 190–193.
7. M. Vukobratovi, B. Borovac, D. Surla and D. Stoki, *Biped Locomotion: Dynamics, Stability, Control, and Application* (Springer-Verlag, Berlin, 1990), pp. 321–330.
8. A. Chu, H. Kazerooni and A. Zoss, On the biomimetic design of the Berkeley lower extremity exoskeleton (BLEEX), in *IEEE Int. Conf. Robotics and Automation (ICRA)* (IEEE Press, Barcelona, Spain, 2006), pp. 4356–4363.
9. G. T. Huang, Demo: Wearable robots, *Tech. Rev.* (July/August, 2004).
10. X. Liu, K. H. Low and H. Y. Yu, Development of a lower extremity exoskeleton for human performance enhancement, in *IEEE Int. Conf. Intelligent Robots and Systems (IROS)*, Sendai, Japan (IEEE Press, 2004), pp. 3889–3894.
11. G. A. Cavagna and M. Kaneko, Mechanical work and efficiency in level walking and running, *J. Appl. Physiol.* **268** (1977) 467–481.
12. S. Mochon and T. A. McMahon, Ballistic walking, *J. Biomech.* **13** (1980) 49–57.
13. H. Geyer, A. Seyfarth and R. Blickman, Compliant leg behaviour explains basic dynamics of walking and running, *Proc. Biol. Sci.* **273**(1603) (2006) 2861–2867.
14. K. Endo, D. Paluska and H. Herr, A quasi-passive model of human leg function in level-ground walking, in *IEEE Int. Conf. Intelligent Robots and Systems (IROS)*, Beijing, China (IEEE Press, 2006), pp. 4935–4939.
15. L. J. Marks and J. W. Michael, Science, medicine, and the future: Artificial limbs, *Brit. Med. J.* **323** (2001) 732–735.

16. W. C. Flowers, A man-interactive simulator system for above-knee prosthetics studies, Ph.D. thesis, Massachusetts Institute of Technology (1972).
17. K. James, R. B. Stein, R. Rolf and D. Tepavic, Active suspension above-knee prosthesis, in *6th Int. Conf. Biomechanical Engineering*, Singapore ed. J. C. Goh (1990), pp. 317–320.
18. I. Kitayama, N. Nakagawa and K. Amemori, A microcomputer controlled intelligent A/K prosthesis, in *Proc. 7th World Congress Int. Society for Prosthetics and Orthotics*, Chicago (1992).
19. S. Zahedi, The results of the field trial of the Endolite Intelligent Prosthesis, in *XII Int. Congress of INTERBOR*, Washington (1993).
20. H. Herr and A. Wilkenfeld, User-adaptive control of a magnetorheological prosthetic knee, *Ind. Robot.* **30** (2003) 42–55.
21. T. McGeer, Passive dynamic walking, *Int. J. Robot. Res.* (1990) 62–82.
22. M. Wisse, Essentials of dynamic walking, analysis and design of two-legged robots, Ph.D. thesis, Technical University of Delft (2004).
23. S. H. Collins and A. Ruina, A bipedal walking robot with efficient and human-like gait, in *IEEE Int. Conf. Robotics and Automation (ICRA)* Barcelona, Spain (IEEE Press, 2005), pp. 1983–1988.
24. H. Herr, C. J. Walsh, D. J. Paluska, A. Valiente and K. Pasch, Exoskeletons for walking and running, US Provisional Application Serial No. 60/736, 929 (2005).
25. C. J. Walsh, Biomimetic design of an under-actuated leg exoskeleton for load-carrying augmentation, M.S. thesis, Massachusetts Institute of Technology (2006).
26. C. J. Walsh, D. Paluska, K. Pasch, W. Grand, A. Valiente and H. Herr, Development of a lightweight, underactuated exoskeleton for load-carrying augmentation, in *IEEE Int. Conf. Robotics and Automation (ICRA)*, Florida, USA (IEEE Press, 2006), pp. 3485–3491.
27. K. N. Gregorczyk, J. P. Obusek, L. Hasselquist, J. M. Schiffman, C. K. Bensel, D. Gutekunst and P. Frykman, The effects of a lower body exoskeleton load carriage assistive device on oxygen consumption and kinematics during walking with loads, in *25th Army Sci. Conf.*, Florida, USA (2006).
28. M. L. Palmer, Sagittal plane characterization of normal human ankle function across a range of walking gait speeds, M.S. thesis, Massachusetts Institute of Technology (2002).
29. V. T. Inman, H. J. Ralston and F. Todd, Kinetics of human locomotion, in *Human Walking*, ed. J. Rose and J. G. Gamble (Williams and Wilkins, Baltimore, 1981), p. 91.
30. C. J. Walsh, K. Pasch and H. Herr, An autonomous, underactuated exoskeleton for load-carrying augmentation, in *IEEE Int. Conf. Intelligent Robots and Systems (IROS)* Beijing, China (IEEE Press, 2006), pp. 1410–1415.
31. E. Harman, K. Han, P. Frykman and C. Pandorf, The effects of backpack weight on the biomechanics of load carriage, USARIEM Technical Report, Natick, MA (2000).
32. C. Hausswirth, A. X. Bigard and J. M. Lechevelier, The Cosmed K4 telemetry system as an accurate device for oxygen uptake measurement during exercise, *Int. J. Sports Med.* **18** (1997) 449–453.
33. J. M. Brockway, Derivation of formulae used to calculate energy expenditure in man, *Hum. Nutr. Clin. Nutr.* **41** (1987) 463–471.
34. T. A. McMahon, G. Valiant and E. C. Frederick, Groucho running, *J. Appl. Physiol.* **62**(6) (1987) 2326–2337.

Conor James Walsh received his B.A.I and B.A. degrees in Mechanical and Manufacturing engineering from Trinity College Dublin, Ireland in 2003 and his M.S. degree in Mechanical Engineering from MIT in 2006. In 2006, he worked at Massachusetts General Hospital on the design of a small robot to aid in the performance of computed tomography guided percutaneous lung biopsies. He is currently a Ph.D. candidate in the Mechanical Engineering Department at MIT. His primary research objective is to develop practical engineering technologies that assist humanity directly such as assistive devices to augment the physical ability of humans and high-tech medical devices to improve patient care. He is particularly interested in how new technological advances in imaging technology can be utilized in the development of new surgical and diagnostic devices.

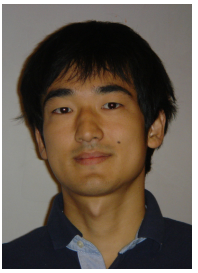

Ken Endo received his B.A. and M.S. degrees in Mechanical Engineering from Keio University, Japan in 2001 and 2003, respectively. There he also worked as a research assistant at the Kitano Symbiotic Systems Project, ERATO, JST in Japan. After graduation, he worked as a researcher at the Future Robotics Technology Center in the Chiba Institute of Technology in Japan. He is currently a Ph.D. student in the Electrical Engineering and Computer Science Department at MIT. His primary research objective is to apply robotics technology to prosthetic knee and ankle systems to assist or augment amputee locomotion.

Hugh Herr received his B.A. degree in Physics from Millersville University of Pennsylvania in 1990, his M.S. degree in Mechanical Engineering from MIT and his Ph.D. in Biophysics at Harvard University in 1998. He is an Associate Professor within MIT's Program of Media Arts and Sciences, and The Harvard-MIT Division of Health Sciences and Technology. His primary research objective is to apply the principles of biomechanics and neural control to guide the designs of prostheses, orthoses and exoskeletons that amplify the endurance and strength of humans.

Hugh Herr is the author of over 60 technical publications, proceedings, editorials and books. He is an active member of IEEE, and was the General Chair of "No Barriers," a conference held in Italy and the US highlighting recent research in permanent assistive devices and therapy tools for physically-challenged people.